# Microscopic stability of cold shock protein A examined by NMR native state hydrogen exchange as a function of urea and trimethylamine *N*-oxide

VICTOR A. JARAVINE, KLARA RATHGEB-SZABO, AND ANDREI T. ALEXANDRESCU[1]

Department of Structural Biology, Biozentrum, University of Basel, Switzerland CH-4056

## Abstract

Native state hydrogen exchange of cold shock protein A (CspA) has been characterized as a function of the denaturant urea and of the stabilizing agent trimethylamine *N*-oxide (TMAO). The structure of CspA has five strands of $\beta$-sheet. Strands $\beta 1$–$\beta 4$ have strongly protected amide protons that, based on experiments as a function of urea, exchange through a simple all-or-none global unfolding mechanism. By contrast, the protection of amide protons from strand $\beta 5$ is too weak to measure in water. Strand $\beta 5$ is hydrogen bonded to strands $\beta 3$ and $\beta 4$, both of which afford strong protection from solvent exchange. Gaussian network model (GNM) simulations, which assume that the degree of protection depends on tertiary contact density in the native structure, accurately predict the strong protection observed in strands $\beta 1$–$\beta 4$ but fail to account for the weak protection in strand $\beta 5$. The most conspicuous feature of strand $\beta 5$ is its low sequence hydrophobicity. In the presence of TMAO, there is an increase in the protection of strands $\beta 1$–$\beta 4$, and protection extends to amide protons in more hydrophilic segments of the protein, including strand $\beta 5$ and the loops connecting the $\beta$-strands. TMAO stabilizes proteins by raising the free energy of the denatured state, due to highly unfavorable interactions between TMAO and the exposed peptide backbone. As such, the stabilizing effects of TMAO are expected to be relatively independent of sequence hydrophobicity. The present results suggest that the magnitude of solvent exchange protection depends more on solvent accessibility in the ensemble of exchange susceptible conformations than on the strength of hydrogen-bonding interactions in the native structure.

**Keywords:** hydrogen bonding; hydrogen exchange; OB-fold; osmolyte; protein folding; protein stabilization; sequence hydrophobicity; two-state folding approximation

Cold shock protein A (CspA) is a 70 residue (7.4 kDa) protein expressed in *Escherichia coli* following a rapid drop in temperature from 37 to 10 °C (Chatterjee et al., 1993; Schindelin et al., 1994; Jiang et al., 1997; Feng et al., 1998). The protein is believed to function as an RNA chaperone, facilitating translation at low temperatures by preventing the formation of mRNA secondary structure (Jiang et al., 1997). The sequence of CspA shows homology to a large number of prokaryotic proteins (Perl et al., 1998) and to the family of eukaryotic Y-box proteins (Wolffe, 1994). The structure of CspA (Schindelin et al., 1994; Feng et al., 1998) consists of a five stranded $\beta$-barrel (Fig. 1) and is assigned in the SCOP classification of protein topologies (Murzin et al., 1995) to the OB-fold motif (Murzin, 1993). This OB-fold motif is found in a large superfamily of nonhomologous proteins that typically share oligonucleotide or oligosaccharide binding functions (Murzin, 1993). Our group has been interested in the extent to which folding and misfolding mechanisms are conserved within structurally related OB-fold proteins (Alexandrescu et al., 1999).

As monitored by circular dichroism (CD) and fluorimetry, cold shock protein homologues from *E. coli*, *Bacillus subtilis*, *Bacillus caldolyticus*, and *Thermotoga maritima* show apparent two-state equilibrium unfolding transitions when denatured by urea or guanidinium hydrochloride (Schindler et al., 1995; Perl et al., 1998; Reid et al., 1998). Indeed, it has been argued that two-state transitions may be typical of "small" proteins (Schindler & Schmid, 1996; Fersht, 1997; Jackson, 1998).

The recently described "native state hydrogen exchange" experiment offers an alternative way to look at protein unfolding. Labile amide protons can be shielded from solvent exchange by protein structure:

$$\text{closed} \underset{k_{cl}}{\overset{k_{op}}{\rightleftharpoons}} \text{open} \overset{k_{int}}{\longrightarrow} \text{exchanged.} \qquad (1)$$

Reprint requests to: Andrei T. Alexandrescu, Department of Molecular and Cell Biology, University of Connecticut, 75 North Eagleville Road U-3125, Storrs, Connecticut 06269-3125; e-mail: andrei@uconnvm.uconn.edu.

[1]Present address: Department of Molecular and Cell Biology, University of Connecticut, 75 North Eagleville Road U-3125, Storrs, Connecticut 06269-3125.
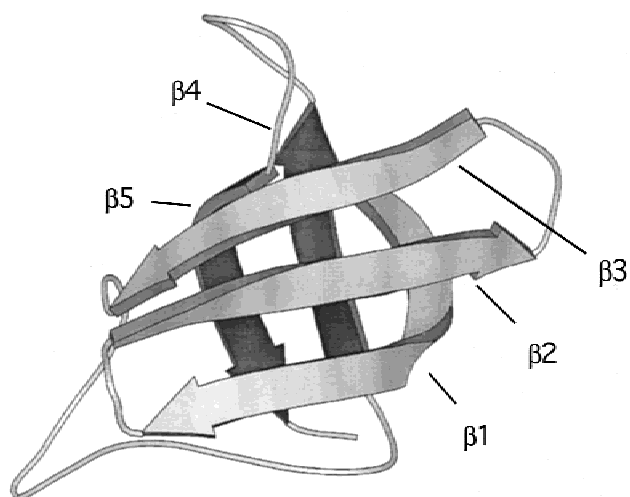
**Fig. 1.** MOLSCRIPT diagram (Kraulis, 1991) of the X-ray structure of CspA (Schindelin et al., 1994). In the X-ray structure, the five strands of $\beta$-sheet correspond to residues 5–13 ($\beta$1), 18–23 ($\beta$2), 30–33 ($\beta$3), 50–56 ($\beta$4), 63–69 ($\beta$5). In the NMR structure (Feng et al., 1998), the limits of strands $\beta$2 and $\beta$5 are slightly different: residues 18–22 and 63–70, respectively. The three stranded $\beta$1–$\beta$3 meander (light gray) and two-stranded $\beta$4-$\beta$5 hairpin (dark gray) fold into a closed five-stranded $\beta$-barrel.

Under conditions that favor the native state, "*closed*" exchange-resistant conformations are in equilibrium with minute concentrations of "*open*" exchange-susceptible conformations, as dictated by the Boltzmann distribution of the system. Since solvent exchange occurs through *open* conformations, these will influence measured exchange rates even when they exist in a background of more than 99% *closed* conformations. Hydrogen exchange can thus be used to probe the stabilities of minutely populated ($\ll 1\%$) partially or completely unfolded species, under conditions that strongly favor the native state. This contrasts with equilibrium unfolding transitions, which require a range of solution conditions such that populations vary between $\sim$5 and $\sim$95% (Bai & Englander, 1996).

It has been pointed out that the native state hydrogen exchange experiment cannot provide information on the pathway of protein folding (Clarke & Fersht, 1996; Clarke et al., 1997; Itzhaki et al., 1997). At the same time, it is becoming increasingly clear that protein folding is a highly heterogeneous process, which is poorly described in terms of a discrete sequence of events (Harrison & Durbin, 1985; Zhou & Wang, 1996; Dill & Chan, 1997). In the absence of a pathway, the distinction between species that are "on-pathway" and "off-pathway" is at best blurred. Perhaps the most direct route toward understanding protein folding is to characterize the thermodynamic determinants of protein structure (Anfinsen, 1973; Tanford, 1978). When coupled to the resolving power of NMR, native state hydrogen exchange offers an unparalleled opportunity to investigate the energetics of protein structure at residue-level resolution (Bai et al., 1995; Chamberlain et al., 1996; Yi et al., 1997; Fuentes & Wand, 1998; Alexandrescu et al., 1999).

To complement the extensive equilibrium and kinetic folding studies of cold shock proteins (Schindler et al., 1995; Perl et al., 1998; Reid et al., 1998), the present work examines the microscopic stability of the *E. coli* CspA by the native state hydrogen exchange method.

## Results

### Protection from solvent exchange

CspA has a low stability to unfolding with a $\Delta G_u(0)$ of $\sim$2.8 kcal/mol at pD 5.4 and 5 °C (where pD is the glass electrode reading of a D$_2$O solution uncorrected for the deuterium isotope effect). The low stability of the protein results in fast hydrogen exchange rates. A previous study established that nearly all of the backbone amide protons of CspA are fully exchanged within 2 h of dissolving the protein in D$_2$O, at pD 6.0 and a temperature of 30 °C (Feng et al., 1998). To minimize intrinsic solvent exchange rates (Bai et al., 1993), the measurements in the present work were performed at lower temperature and more acidic pD. Figure 2A shows an $^1$H-$^{15}$N heteronuclear single quantum coherence (HSQC) spectrum of CspA in H$_2$O, at pH 5.4 and a temperature of 5 °C. Under these conditions, 58 of the 67 backbone $^1$H–$^{15}$N correlations expected from the amino acid sequence of CspA are resolved and can be used as site-specific probes of solvent exchange. On dissolving the protein in D$_2$O, 21 (36%) of the resolved correlations persist for at least 30 min (Fig. 2B), and 9 persist for longer than 1 day. The number of amide protons protected after 30 min increases to 35 (60%) in the presence of 0.2 M TMAO (Fig. 2C), an osmolyte that has been shown to stabilize proteins to denaturation (Lin & Timasheff, 1994; Wang & Bolen, 1997; Baskakov & Bolen, 1998; Baskakov et al., 1999). Increased protection from solvent exchange has been previously described for proteins in the presence of the osmolytes sucrose and glycine (Wang et al., 1995; Foord & Leatherbarrow, 1998).

Hydrogen bonds in the X-ray structure of CspA (Schindelin et al., 1994) were identified using cutoff criteria of an amide proton to acceptor distance of less than 2.5 Å; and an N-H-acceptor angle greater than 120°. Based on these criteria, 44 of the backbone amide protons in CspA (66%) serve as hydrogen bond donors. Of these, 21 (48%) are protected in D$_2$O, and 33 (75%) are protected in D$_2$O solutions containing 0.2 M TMAO. With the possible exception of Lys50, whose $^1$H–$^{15}$N correlation overlaps with that of Val9, all of the amide protons protected in D$_2$O are involved in hydrogen bonds. Of the additional amide protons protected in the presence of TMAO, those of Lys28, Asp29, and Leu45 do not participate in hydrogen bonds.

### Exchange mechanism

Experimentally determined hydrogen exchange rates ($k_{obs}$) depend on closing ($k_{cl}$), opening ($k_{op}$), and intrinsic ($k_{int}$) rates of exchange (Equation 1). Intrinsic exchange rates are influenced by factors such as solution pD, temperature, amino acid type, and sequence neighbors. These can be modeled from a database of exchange rates for small unstructured peptides (Bai et al., 1993). Under native conditions ($k_{op} \ll k_{cl}$), and assuming that the concentration of *open* conformation is at steady state, the observed exchange rate is given by

$$k_{obs} = \frac{k_{op} k_{int}}{(k_{cl} + k_{int})}. \tag{2}$$

In the *EX1* limit ($k_{cl} \ll k_{int}$),
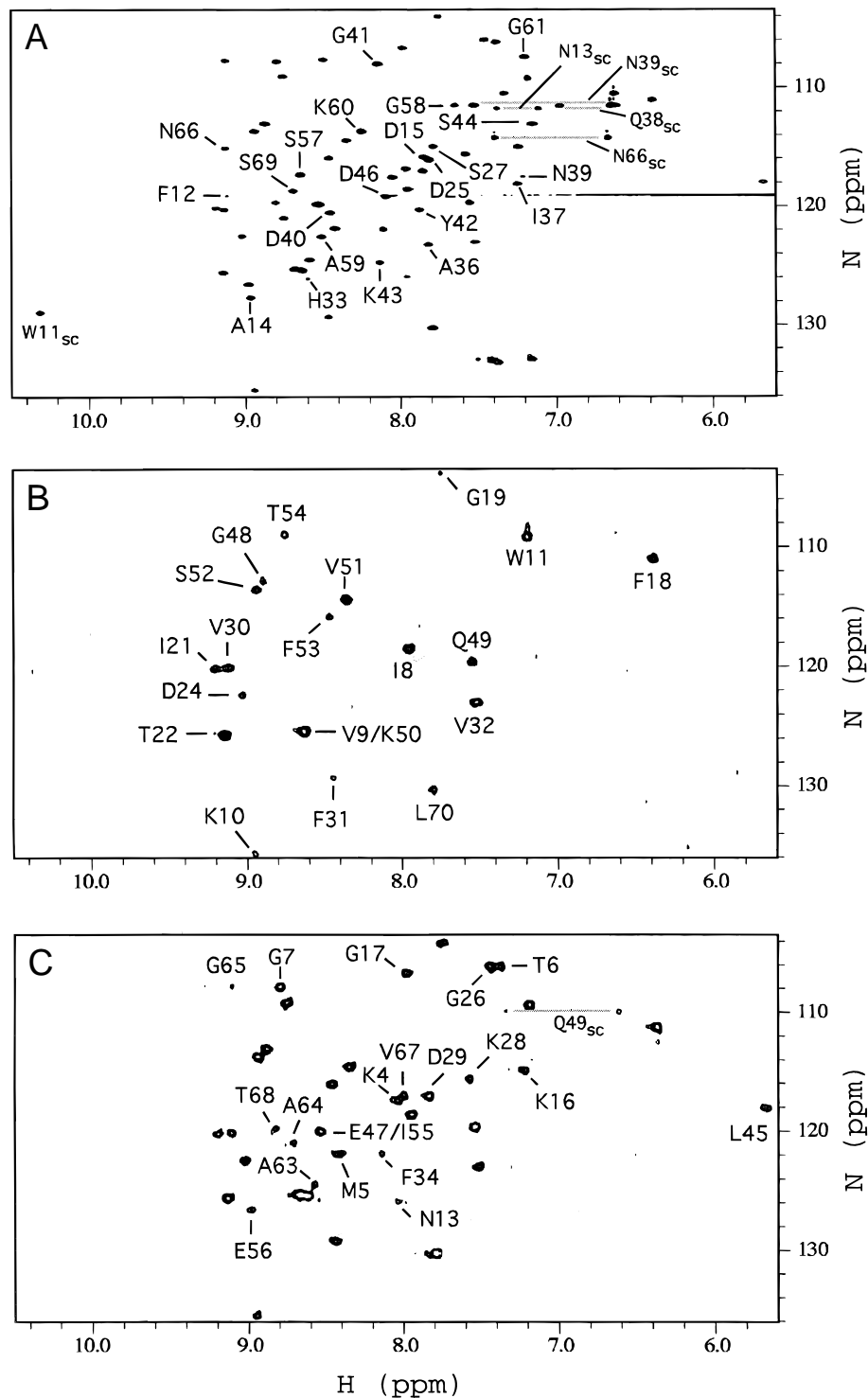
$$k_{obs} = k_{op} \tag{3}$$

**Fig. 2.** $^1H$–$^{15}N$ HSQC spectra of CspA illustrating amide protons protected from solvent exchange. **A:** CspA in $H_2O$ at pH 5.4. **B:** Freshly dissolved CspA after 30 min of exchange in $D_2O$ at pD 5.4. **C:** Freshly dissolved CspA after 30 min of exchange in a $D_2O$ solution containing 0.2 M TMAO, pD 5.4. Amide protons that are not protected in either $D_2O$ or $D_2O$/TMAO are labeled in **A**. Amide protons protected in $D_2O$ are labeled in **B**. Protons that only become strongly protected in the presence of 0.2 M TMAO are labeled in **C**. Residues Gly7, Gly17, and Phe20 are marginally protected in $D_2O$ and are observed at lower contour levels in the spectrum shown in **B**.

and the observed rates are limited by the rates of the *opening* reactions.

In the *EX2* limit ($k_{int} \ll k_{cl}$),

$$k_{obs} = \left(\frac{k_{op}}{k_{cl}}\right)k_{int} \tag{4}$$

and the observed rates are proportional to the equilibrium constants relating the concentrations of *open* and *closed* conformations. In turn, these can be related to the free energy differences between open and closed conformations

$$\Delta G_{HX} = -RT \ln\left(\frac{k_{obs}}{k_{int}}\right). \tag{5}$$

Above pD ~ 4, the logarithm of $k_{int}$ is linearly proportional to pD. If protein stability is invariant over the pD range studied, solvent exchange rates measured at different pD values can be used to determine if *EX1* or *EX2* exchange mechanisms predominate (Bai et al., 1993; Clarke & Fersht, 1996; Yi et al., 1997).

Figure 3A shows a linear regression of $\log(k_{obs})$ values obtained for CspA in $D_2O$ at pD 5.4 and 7.2. Because the mechanism of exchange can shift from the *EX2* to *EX1* with increasing concentration of denaturant, as protein stability and folding rates decrease (Clarke & Fersht, 1996; Yi et al., 1997; Fuentes & Wand, 1998), the pD dependence of exchange was also measured in the presence of 1.5 M urea (Fig. 3B), the highest concentration of denaturant used in this study. The slope of the linear regressions for the samples in both water and 1.5 M urea are close to unity. The observed differences in hydrogen exchange rates, however, are less than expected for an *EX2* mechanism, where the logarithm of $k_{obs}$ should increase linearly with pD. The y-intercept for the data in water is $-1.4 \pm 0.2$, whereas the difference in pDs predicts a value of $-1.8$ (Fig. 3A). Similarly, the y-intercept of $-0.3 \pm 0.6$ for the protein in 1.5 M urea is lower than the $-1.2$ difference in pD values (Fig. 3A). The discrepancies could be due to *EX1* exchange, where $k_{obs}$ will tend to be independent of $k_{int}$ and constant as a function of pD (Equation 3). Alternatively, the assumption that protein stability is invariant as a function of pD may be invalid.

Figure 3C demonstrates that the stability of CspA to urea denaturation decreases with decreasing pD. Similar decreases with decreasing pD were observed for the stability of the protein to thermal denaturation (not shown). The equilibrium unfolding transition for CspA in 99.8% $D_2O$ at pD 7.2, gives a $\Delta G_u(0)$ of $3.9 \pm 0.4$ kcal/mol (Table 1). At pD 5.4, $\Delta G_u(0)$ decreases by about 1 kcal/mol compared to pD 7.2 (Table 1). The increase in $k_{obs}$ expected for *EX2* exchange due to the larger value of $k_{int}$ at higher pH is partially compensated by the smaller concentration of exchange susceptible denatured molecules on raising the pD from 5.4 to 7.2 (Equations 4, 5).

The use of the pD dependence of exchange rates to distinguish between *EX1* and *EX2* mechanisms is precluded by the pD dependence of the stability of CspA. A number of considerations, however, strongly suggest that exchange at pD 5.4 and 5°C is in the *EX2* limit. First, in contrast to the data in Figure 3B, a plot of $\log(k_{obs})$ at pD 5.4 and 7.2 for CspA in 1.5 M urea gives a slope of 0.07 (not shown). This is consistent with an *EX2* mechanism at pD 5.4 in the presence of 1.5 M urea, which switches to *EX1* only at higher pD values between 6.5 and 7.2. Second, the $\Delta G_u(0)$ values for the most slowly exchanging amide protons in strands

$\beta 1$–$\beta 4$, obtained from hydrogen exchange measurements as a function of both urea and TMAO at pD 5.4, match those determined from equilibrium unfolding. In spite of disparate $k_{int}$ values, the most slowly exchanging amide protons give uniform $\Delta G_u(0)$ values, an observation inconsistent with *EX1* exchange (Bai et al., 1995). Finally, stopped flow fluorescence measurements indicate that the refolding of CspA from urea is extremely fast (Reid et al., 1998). At pH 7.0 and 25°C, the folding rates of CspA were estimated to be 188 $s^{-1}$ in $H_2O$ and 67 $s^{-1}$ in the presence of 1.5 M urea (Reid et al., 1998). For comparison, the highest intrinsic rate calculated for CspA at pD 5.4 and 5°C is 0.1 $s^{-1}$. Assuming similar folding kinetics for the present conditions; $k_{int}$ is at least four orders of magnitude slower than $k_{cl}$ in the absence of denaturant, and at least three orders of magnitude slower than $k_{cl}$ in the presence of 1.5 M urea.

*Magnitude of protection in the absence and presence of TMAO*

Figure 4A summarizes $\Delta G_{HX}$ values calculated from Equation 5 under the assumption of *EX2* exchange. The first four strands of $\beta$-sheet show uniformly high $\Delta G_{HX}$ values of $3.4 \pm 0.2$ kcal/mol (mean $\pm$ standard deviation). The only two amide protons that show significantly lower $\Delta G_{HX}$ values are Asp24 in the loop between strands $\beta 2$ and $\beta 3$, and Leu70 the C-terminus at the end of strand $\beta 5$. The two residues have the tenth lowest and lowest intrinsic exchange rates in the protein, respectively. This observation suggests a stability threshold, below which the measurement of solvent exchange protection is precluded by fast intrinsic exchange rates. Except for Leu70, amide protons in strand $\beta 5$ show no detectable protection from solvent exchange in water. In retrospect, the pattern of protection observed in this work is very similar to that reported for CspA at pD 6.0 and 30°C [cf. Fig. 3 of Feng et al. (1998)]. At the higher pD and temperature, most amide protons from strands $\beta 1$–$\beta 4$ were protected, however, in strand $\beta 5$ protection was only detected for Leu70 (Feng et al., 1998).

The $\Delta G_{HX}$'s for the subset of amide protons protected in water (Fig. 4A) increases by $0.5 \pm 0.1$ kcal/mol in the presence of 0.2 M TMAO (Fig. 4B). Furthermore, protection is observed for additional amide protons from residues in strand $\beta 5$ and in the loops flanking the $\beta$-strands. The majority of amide protons for which protection can only be measured in the presence of TMAO gives lower $\Delta G_{HX}$ values than those protected in the absence of TMAO. This suggests that as TMAO stabilizes the protein, there is an increase in the proportion of amide protons whose exchange is sufficiently slowed to enable a quantitative determination of protection.

*Solvent exchange in relation to native structure and sequence hydrophobicity*

Figure 4D shows simulated $\Delta G_{HX}$ values, calculated from the X-ray (Schindelin et al., 1994) and NMR (Feng et al., 1998) structures of CspA using the Gaussian network model (GNM) algorithm (Bahar et al., 1998). The GNM formalism models fluctuations about the mean native conformation of a protein. Fluctuations are assumed to depend only on the distribution of tertiary contacts within 7 Å. Interactions between residue pairs are assumed to be homogeneous, to obey a harmonic potential, and to have a uniform force constant $\gamma$ regardless of residue type. The term $\gamma$ thus becomes an adjustable parameter that can be used to scale simulated values
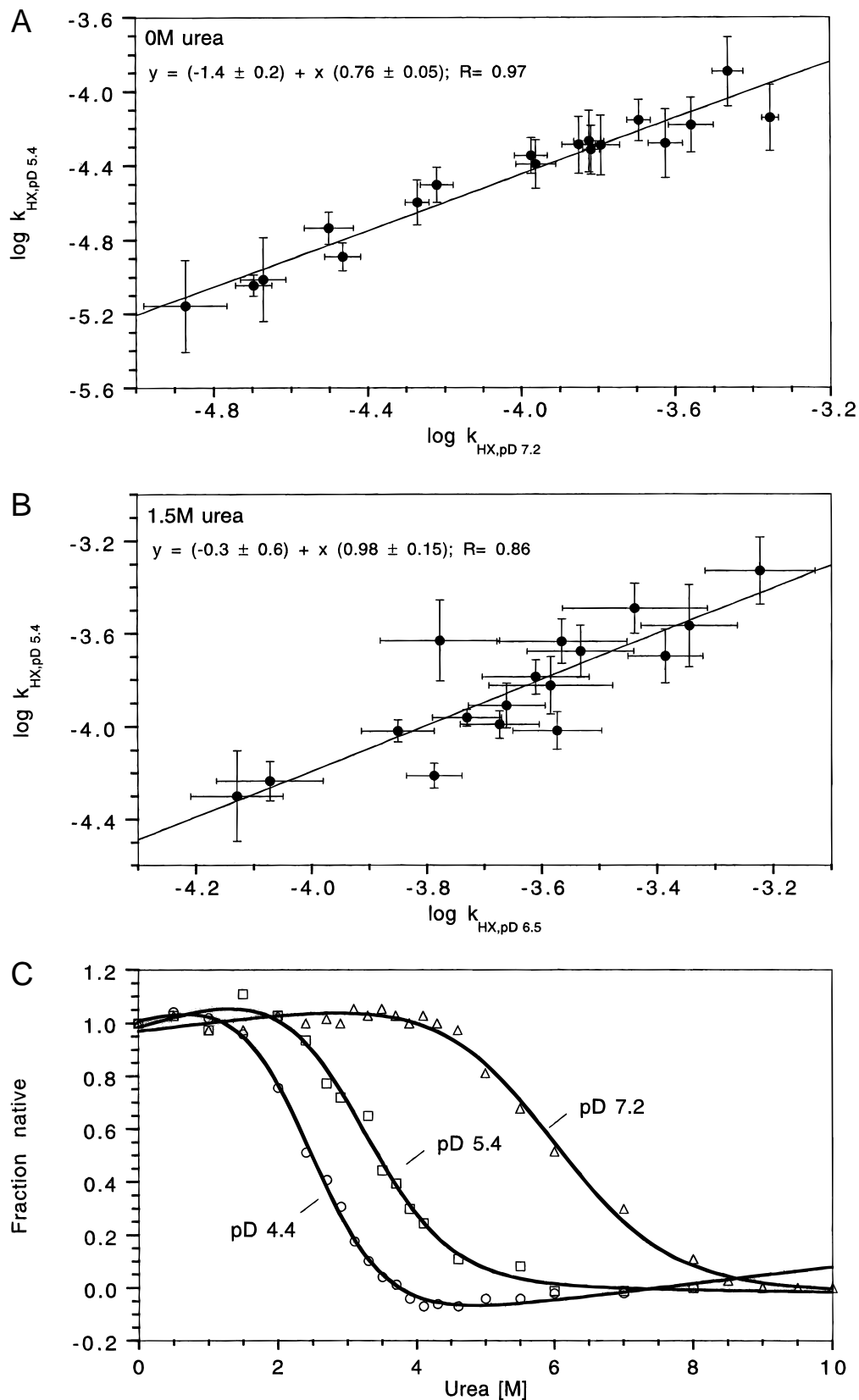
**Fig. 3.** Dependence of exchange rates and equilibrium unfolding transitions on solution pD. **A:** Plot of $\log(k_{HX})$ at pD 5.4 and 7.2 for CspA in $D_2O$. **B:** Plot of $\log(k_{HX})$ at pD 5.4 and 6.5 for CspA in $D_2O$ containing 1.5 M urea. Each data point corresponds to an individual residue. **C:** Urea-induced equilibrium unfolding transitions monitored by ellipticity at 222 nm for CspA in 99.8% $D_2O$ at three pD values. All experiments are at 5 °C. The curves represent fits of the equilibrium unfolding data to a two state denaturation model (Pace, 1986). Values for $[urea]_{1/2}$, $m$, and $\Delta G_u(0)$ obtained from the fits are given in Table 1.

**Table 1.** *The pD dependence of the midpoint, m, and $\Delta G_u(0)$ values for urea denaturation of CspA in 99.8% D$_2$O, followed by CD at 5°C*

| pD | [urea]$_{1/2}$ (M) | $m$ (kcal mol$^{-1}$ M$^{-1}$) | $\Delta G_u(0)$ (kcal mol$^{-1}$) |
|---|---|---|---|
| 7.2 | 5.9 ± 0.1 | 0.7 ± 0.1 | 3.9 ± 0.4 |
| 5.4 | 3.1 ± 0.2 | 0.9 ± 0.2 | 2.8 ± 0.5 |
| 4.4 | 2.4 ± 0.1 | 1.0 ± 0.1 | 2.4 ± 0.2 |

with respect to the experimental data (Bahar et al., 1998). The GNM approach has been successfully used to model crystallographic *B* factors, as well as $\Delta G_{HX}$ values of five proteins (Bahar et al., 1998). When applied to CspA, the GNM approach accurately predicts uniformly high stabilities to hydrogen exchange for strands

$\beta1$–$\beta4$ but fails to predict the lack of protection for strand $\beta5$. The results in 0.2 M TMAO (Fig. 4B) are more consistent with the GNM simulations, although experimental $\Delta G_{HX}$ values for strand $\beta5$ remain lower than predicted.

The hydrophobicity profile of the CspA sequence is shown in Figure 4C. The most hydrophobic segment of the protein corresponds to residues Phe34–Ile37, which in the native structure is downstream of strand $\beta3$ (see also Alexandrescu & Rathgeb-Szabo, 1999). The high sequence hydrophobicity of this segment is not reflected in unusually high $\Delta G_{HX}$ values. The least hydrophobic segment involved in the regular secondary structure of the protein is strand $\beta5$, with a positive peak area nearly half that of any of the other four $\beta$-strands in the protein.

### Dependence of exchange on urea and TMAO concentration

An opening reaction productive for solvent exchange can take the form of a noncooperative local fluctuation, which only affects the immediate vicinity of a given amide proton, a cooperative partial
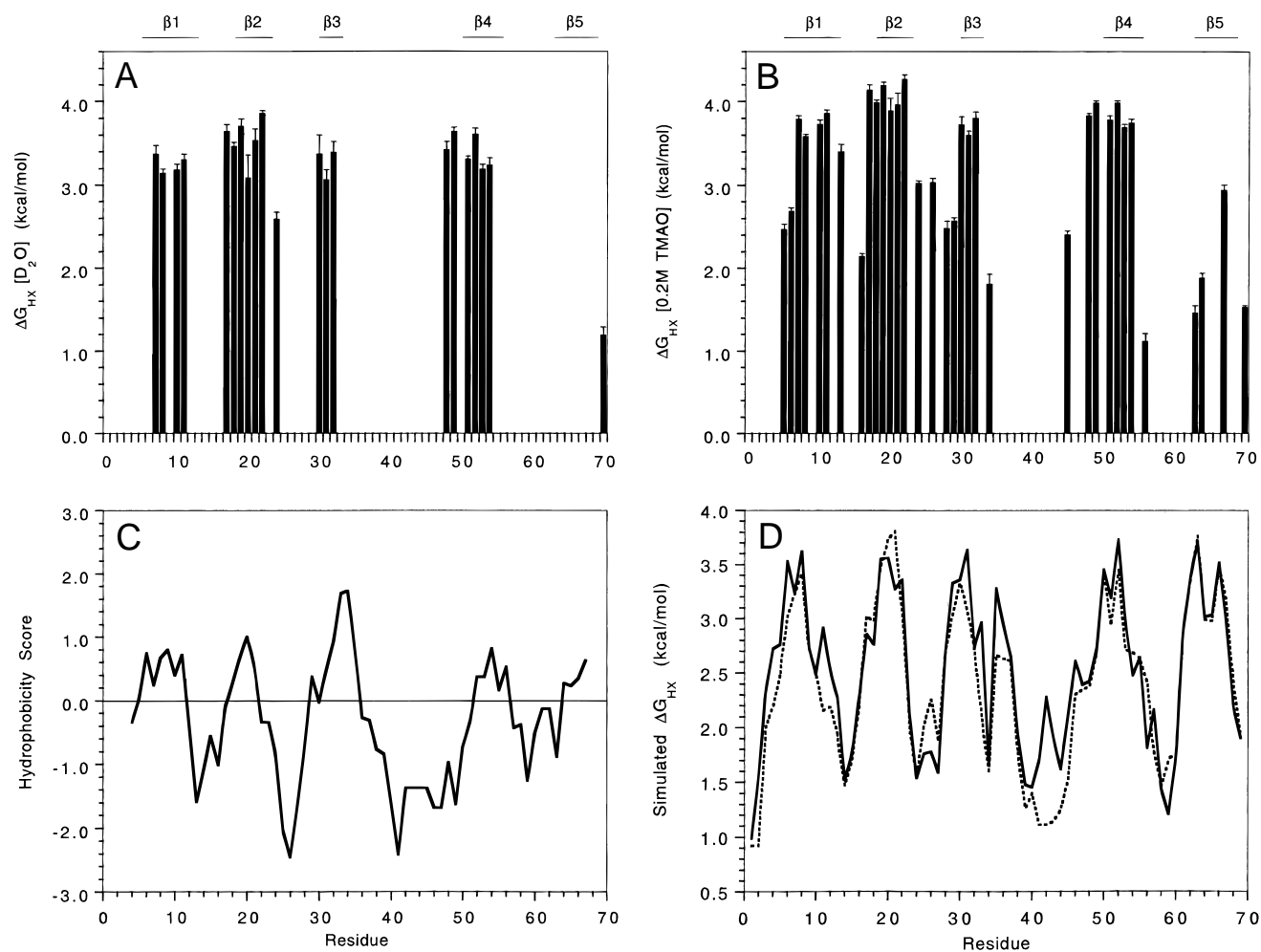


**Fig. 4.** Measured and simulated hydrogen exchange protection and sequence hydrophobicity. **A:** Experimental $\Delta G_{HX}$ values for CspA in D$_2$O. **B:** Experimental $\Delta G_{HX}$ values for CspA in a D$_2$O solution containing 0.2 M TMAO. **C:** Kyte and Doolittle (1982) hydrophobicity profile for the CspA sequence. Positive and negative values indicate hydrophobic and hydrophilic scores, respectively. **D:** Simulated $\Delta G_{HX}$ values calculated by application of the GNM algorithm (Bahar et al., 1998) to the crystal (solid line) and NMR (dashed line) structures of CspA (Schindelin et al., 1994; Feng et al., 1998). The horizontal bars at the top of each plot indicate the sequence positions of the $\beta$-strands in the X-ray structure of CspA (Schindelin et al., 1994).

unfolding of a segment of the protein, or a complete "global" unfolding transition. Localized noncooperative opening reactions expose little new surface to denaturant. Consequently, protection from solvent exchange will show little dependence on denaturant concentration. Cooperative subglobal or global opening reactions expose moderate to large amounts of surface to denaturant. Accordingly, solvent exchange through these mechanisms will be promoted with increasing concentration of denaturant. The dependence of native state hydrogen exchange on denaturant concentration can be used to ascertain the cooperativities of the opening reactions responsible for exchange. If the dominant contributions to exchange are from cooperative partial or complete unfolding reactions, $\Delta G_{HX}$ has a linear dependence on denaturant concentration

$$\Delta G_{HX} = \Delta G_u(0) - (m * [D]) \qquad (6)$$

where $\Delta G_u(0)$ is the change in free energy of unfolding extrapolated to zero concentration of denaturant, and the *m*-value describes the slope of the denaturant concentration dependence of $\Delta G_{HX}$. For some protons, exchange is initially invariant at low concentrations of denaturant and increases at high concentrations (Bai et al., 1995; Chamberlain et al., 1996). To treat these cases, $\Delta G_{HX}$ is modeled to contain contributions from two types of exchange mechanisms:

$$\Delta G_{HX} = -RT \ln \left( \exp \left( -\frac{\Delta G_f}{RT} \right) \right.$$
$$\left. + \exp \left[ \frac{((m * [D]) - \Delta G_u(0))}{RT} \right] \right). \qquad (7)$$

$\Delta G_f$ is associated with noncooperative denaturant-independent fluctuations. The previously described $\Delta G_u(0)$ term is associated with cooperative unfolding processes that are promoted with denaturant.

Figure 5A shows plots of $\Delta G_{HX}$ as a function of urea for four representative protons in CspA. Of the 19 protons that were amenable to analysis, 18 showed a linear decrease of $\Delta G_{HX}$ with increasing concentration of urea, described by the simpler model of Equation 6. The sole exception Phe31 is better fit by the model of Equation 7, with a $\Delta G_f$ of $3.2 \pm 0.2$ kcal/mol and a $\Delta G_u(0)$ of $4.0 \pm 0.4$ kcal/mol. A similar predominance of linear dependencies for acid denatured RNaseH has been attributed to the "molten globule" character of this species (Chamberlain & Marqusee, 1998). The present results suggest that the observation of a single type of exchange mechanism (Equation 6) may be a consequence of a low stability to unfolding (3 kcal/mol for CspA and 4 kcal/mol for acid denatured RNaseH).

Figure 5B shows plots of the TMAO concentration dependence of $\Delta G_{HX}$. The subset of amide protons that are strongly protected in D$_2$O (Fig. 4A) show a linear increase of $\Delta G_{HX}$ from $3.4 \pm 0.2$ kcal/mol in the absence of TMAO to a maximum of $4.3 \pm 0.2$ kcal/mol in the presence of 0.5 M TMAO. Further increases in TMAO concentration lead to a plateau at ~0.6 M, followed by decreases in $\Delta G_{HX}$ values by 1 M TMAO (not shown). At this time, the effects of high TMAO concentrations have not been examined in detail, and the analysis presented here is limited to the linear increases in $\Delta G_{HX}$ observed up to 0.5 M TMAO.

### Free energy changes and cooperativities of opening reactions

Figures 6A and 6C summarize $\Delta G_u(0)$ and *m*-values obtained from least-squares fits of decreases in $\Delta G_{HX}$ values with increasing con-

centration of the denaturant urea (Equation 6). Figures 6B and 6D summarize $\Delta G_u(0)$ and *m*-values obtained from fits of increases in $\Delta G_{HX}$ values with increasing concentration of the stabilizing agent TMAO (Equation 6). The black columns in Figures 6B and 6D correspond to amide protons from strands $\beta 1$–$\beta 4$ that are strongly protected in the absence of TMAO. For these amide protons, it was possible to characterize both the urea and TMAO dependence of hydrogen exchange. Due to the linear dependence of $\Delta G_{HX}$ (Fig. 5), extrapolation from urea or TMAO gives very similar values for $\Delta G_u(0)$, the change in free energy in the absence of additives. The magnitudes of the slopes (*m*-values) obtained from the TMAO titrations (Fig. 6D) are about twice as large as those from the urea titrations (Fig. 6C). This observation is likely to reflect that on a molar basis the stabilizing effects of TMAO are twice as large as the destabilizing effects of urea (Lin & Timasheff, 1994).

The red columns in Figures 6B and 6D correspond to amide protons that were too weakly protected to enable the characterization of the urea dependence of $\Delta G_{HX}$. Small $\Delta G_{HX}$ values could reflect susceptibility to exchange through local fluctuations, or through unfolding. In analogy to the analysis of the effects of denaturants on hydrogen exchange (Bai et al., 1995; Chamberlain et al., 1996), the two mechanisms can be distinguished from the cooperativity of the dependence of $\Delta G_{HX}$ on the concentration of the stabilizer TMAO. Localized noncooperative fluctuations, accompanied by only small changes in surface exposed to solvent, should be relatively independent of TMAO concentration. By contrast, cooperative subglobal or global opening reactions that expose moderate to large new surface area to solvent should give large increases in $\Delta G_{HX}$ with increasing TMAO concentration (large negative *m*-values). Phe34 and Leu45 have *m*-values close to zero. Most of the remaining weakly protected (*red*) amide protons, however, have *m*-values that are close to those of the strongly protected (*black*) amide protons, which exchange through a cooperative global unfolding mechanism (Fig. 6D). This observation is more consistent with small $\Delta G_u(0)$'s for the weakly protected residues than small $\Delta G_f$'s (Equation 7). The $\Delta G_u(0)$ values obtained from extrapolation of the TMAO data to 0 M TMAO are $1.1 \pm 0.7$ kcal/mol smaller for the *red*, compared to the strongly protected *black* amide protons (Fig. 6B). In the absence of TMAO, the stabilities of exchange-resistant conformations for the weakly protected *red* amide protons appear to be so low that exchange is complete on time scales comparable to the dead times of the NMR experiments.

### Discussion

#### Global unfolding of strands $\beta 1$–$\beta 4$, subglobal unfolding of loops and strand $\beta 5$

The first four strands of the CspA $\beta$-sheet give uniformly large $\Delta G_u(0)$ and *m*-values for urea-induced unfolding reactions monitored by native state hydrogen exchange (Fig. 6A,C). The $\Delta G_{HX}$ values for strands $\beta 1$–$\beta 4$ are in good agreement with the $\Delta G_u(0)$ value of $2.8 \pm 0.5$ kcal/mol obtained for equilibrium unfolding monitored by circular dichroism (Fig. 3C). There are two prolines in CspA. The *cis* and *trans* proline isomers will not reach their equilibrium populations in hydrogen exchange experiments (Bai et al., 1994). Assuming that the ratio of *cis*:*trans* isomers in unfolded CspA is 1:4, this effect will overestimate $\Delta G_{HX}$ by 0.25 kcal/mol relative to the $\Delta G_u(0)$ values measured in equilibrium unfolding transitions (Bai et al., 1994). Including this correction further improves the agreement between the largest $\Delta G_u(0)$ values
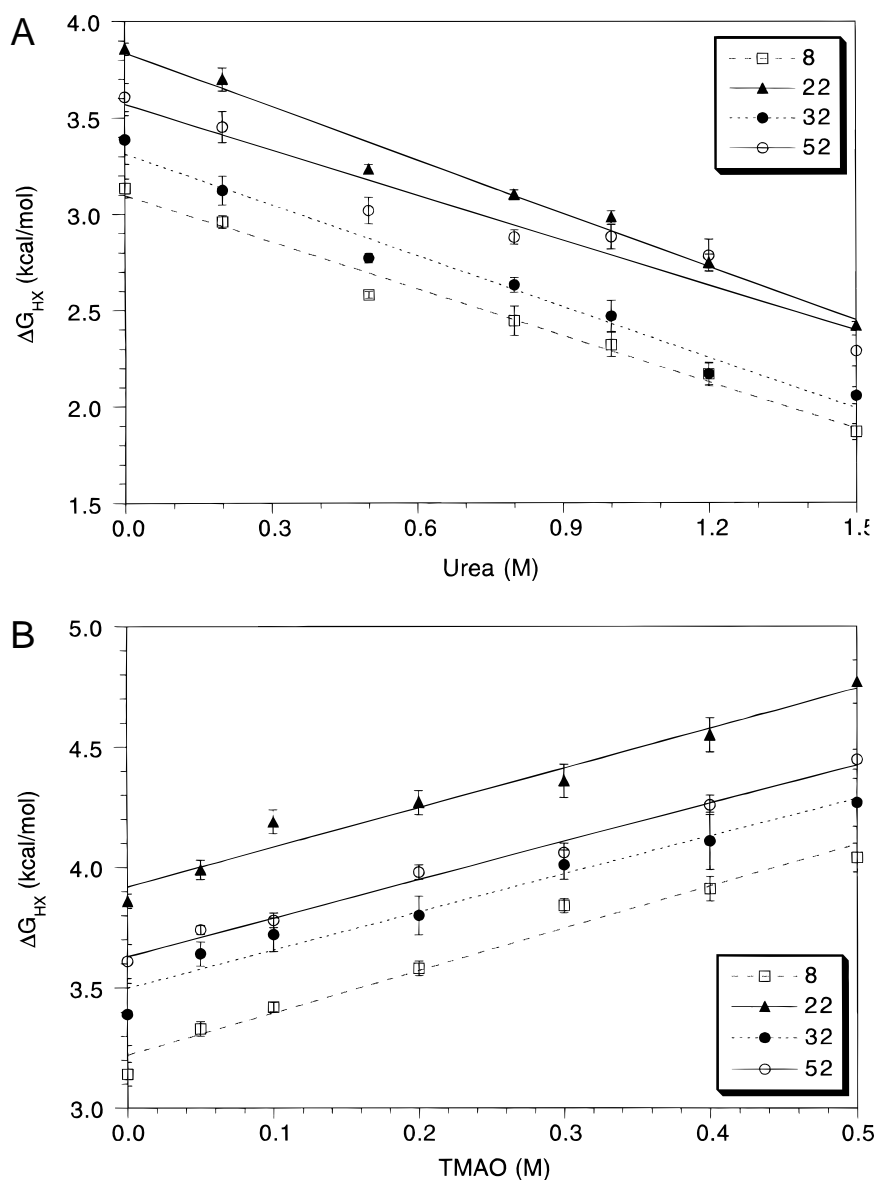
**Fig. 5.** $\Delta G_{HX}$ as a function of (**A**) urea and (**B**) TMAO concentration. Representative residues from each of the first four strands of the CspA β-sheet are shown.

measured from hydrogen exchange and equilibrium unfolding. These observations suggest that amide protons from strands β1–β4 exchange through an all-or-none global unfolding mechanism.

With the exception of Leu70, amide protons from strand β5 show no measurable protection in the absence of TMAO. The lack of protection signifies that the free energy changes for opening reactions that promote exchange are small. These opening reactions could represent noncooperative fluctuations, or more cooperative partial unfolding transitions. Purely localized fluctuations seem an unlikely source for the equally weak protection of all amide protons in strand β5. GNM simulations (Bahar et al., 1998) predict that strand β5 should be no more susceptible to conformational fluctuations about the native structure than strands β1–β4 (Fig. 4D). Protection of amide protons from strand β5 becomes detectable in the presence of TMAO. The *m*-values, describing the

magnitude of the TMAO dependence of $\Delta G_{HX}$, are similar for strands β1–β4 and β5 (Fig. 6D). In analogy to the interpretation of the effects of denaturants on hydrogen exchange (Equations 6, 7), large negative *m*-values suggest a cooperative stabilization of amide protons to hydrogen exchange in the presence of TMAO. In contrast to the *m*-values, the $\Delta G_u(0)$ values for strand β5 are ~2 kcal/mol lower than those for strands β1–β4. Taken together, these observations suggest that the small protection of amide protons in strand β5 reflects a low free energy barrier to segmental unfolding.

Interestingly, the amide protons of residues in the loops between the β-strands show similar behavior (Fig. 6B,D). These residues give lower $\Delta G_u(0)$'s, together with *m*-values that are comparable to those of strands β1–β4. As with strand β5, this suggests that exchange from these residues is cooperative and that the free en-
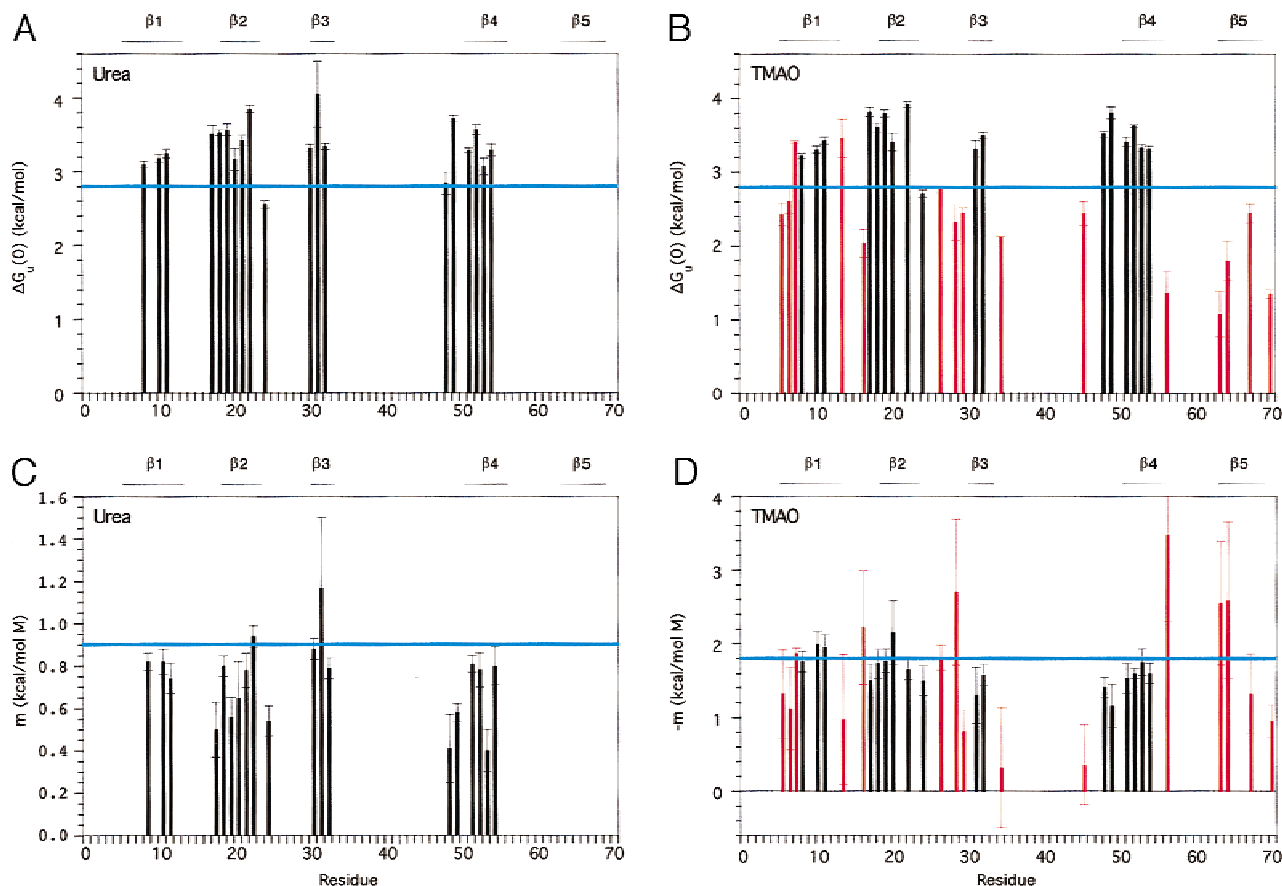
**Fig. 6.** Thermodynamic parameters for CspA unfolding reactions from hydrogen exchange measurements as a function of (**A,C**) urea and (**B,D**) TMAO. Note that the *m*-values in **D**, which describe stabilization to hydrogen exchange as a function of increasing TMAO concentration, have a negative sign (see Fig. 5B; Equation 6). Black columns indicate strongly protected residues. For these residues, exchange could be monitored both as a function of urea and TMAO. The red columns in **B,D** indicate weakly protected residues whose exchange could only be characterized as a function of TMAO. The horizontal blue lines in **A,B,C** indicate parameters obtained from the urea-induced equilibrium unfolding transitions of CspA in $D_2O$, measured by circular dichroism (222 nm) at 5 °C and pD 5.4 (Table 1). The horizontal blue line in **D** is the *m*-value obtained from the equilibrium unfolding transition at pD 5.4, multiplied by a factor of −2.

ergy changes for opening reactions that promote exchange are smaller than those for global unfolding.

At pH 2.0, acid denatured CspA self-assembles into polymers with morphologies similar to those of amyloid fibrils (Alexandrescu & Rathgeb-Szabo, 1998, 1999). Part of the motivation for the present study was to see if native state hydrogen exchange experiments could provide information on partially folded forms of CspA, which might be involved in fibril formation. The exponential growth phase of fibril formation is associated with decreases in $^{15}N$ T2's of residues from the N-terminal half and increases in the $^{15}N$ T2's of residues from the C-terminal half of CspA. These effects were interpreted as a restriction in the mobility of the N-terminal half of the protein upon intermolecular mispairing of the $\beta1$–$\beta3$ meander; concomitant with an increase in the flexibility of the C-terminal half of the protein encompassing the $\beta4$–$\beta5$ hairpin (Alexandrescu & Rathgeb-Szabo, 1999). The present results indicate that strand $\beta5$ is susceptible to subglobal unfolding. Strand $\beta4$, however, appears to exchange only through a global unfolding mechanism together with strands $\beta1$–$\beta3$. The present data do not rule out the possibility that unfolding mechanisms could differ between neutral and acidic pH.

*Magnitude of solvent exchange protection in relation to hydrogen bonding*

There is a strong correspondence between amide protons that are protected from solvent exchange and amide protons that are hydrogen bond donors in the native structure of CspA. All of the amide protons that persist in $D_2O$ (Fig. 2A) are involved in hydrogen bonds. The degree of protection from solvent exchange, however, is poorly correlated with hydrogen-bonding. Hydrogen-bonded amide protons in the hydrophobic strands $\beta1$–$\beta4$ are strongly protected, while hydrogen-bonded amide protons in strand $\beta5$, and in the hydrophilic loops, show no detectable protection in water. In the native structure of CspA, strand $\beta5$ is involved in an antiparallel interaction with strand $\beta4$ and in an irregular parallel interaction with strand $\beta3$. For simplicity, only the hydrogen-bonding network between strands $\beta4$ and $\beta5$ is considered (Fig. 7). The residues in strand $\beta5$ show uniformly weak protection. The residues in strand $\beta4$ show strong protection. The sole exception is the last residue in strand $\beta4$, Glu56. The different degrees of protection for amide protons in strands $\beta4$ and $\beta5$ are difficult to reconcile in terms of the native structure of CspA. A cooperative
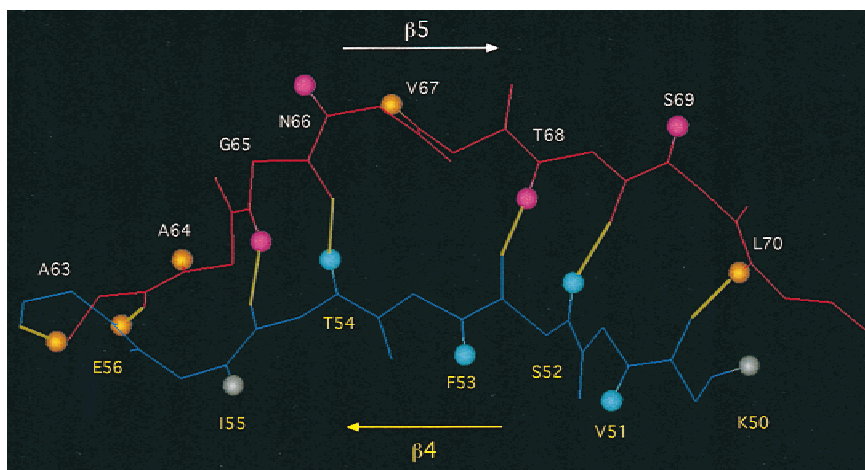
**Fig. 7.** Hydrogen bond network connecting strands $\beta4$ and $\beta5$ in the X-ray structure of CspA (Schindelin et al., 1994). Strand $\beta4$ forms an additional antiparallel interaction with the N-terminal half of strand $\beta1$. Strand $\beta5$ forms an additional short irregular parallel interaction with strand $\beta3$. HN protons are shown as spheres and are color coded according to $\Delta G_u(0,TMAO)$ values (Fig. 6B): blue, strong protection; orange, moderate protection; pink, protection too weak to quantitate, or no protection. The extent of protection for the amide protons of Lys50 and Ile55 (gray) could not be determined because of NMR signal overlap (Fig. 2C).

segmental unfolding of strand $\beta5$, or for that matter less cooperative local fluctuations, should transiently disrupt the hydrogen bonding network between strands $\beta4$ and $\beta5$ (Fig. 7). If protection from solvent exchange were exclusively a function of hydrogen bonding, amide protons from $\beta4$ that are hydrogen bond donors for carbonyl acceptors on $\beta5$ should show weaker protection reflecting the lower stability of strand $\beta5$. In fact, most amide protons in strand $\beta4$ show uniformly strong protection (Figs. 4A, 6B, 7), regardless of whether they are hydrogen-bond donors for strand $\beta1$ (Gly48, Val51, Phe53), for strand $\beta5$ (Ser52, Thr54), or for a reverse turn (Gln49 HN to Asp46 CO). The extent of protection appears to be more closely related to sequence hydrophobicity (Fig. 4C) than to hydrogen-bonding interactions in the native structure. A similar agreement between protection and sequence hydrophobicity, and lack of a correspondence with hydrogen-bonding partners, has been noted for the OB-fold protein LysN (Alexandrescu et al., 1999).

*Stabilization against solvent exchange
in the presence of TMAO*

Small organic osmolytes are accumulated by plants, animals, and microorganisms to maintain cellular osmotic balance (Yancey et al., 1982). In some cartilaginous fish, urea is present at concentrations as high as 0.4 M (Lin & Timasheff, 1994; Wang & Bolen, 1997). To counteract the deleterious effects of urea on protein stability, these fish accumulate a second set of nitrogenous osmolytes, including TMAO (Lin & Timasheff, 1994; Liu & Bolen, 1995; Wang & Bolen, 1997). The physiological ratio of urea:TMAO in fish, such as sharks and rays, is typically between 3:2 and 2:1 (Yancey et al., 1982; Lin & Timasheff, 1994; Wang & Bolen, 1997). The stabilizing effects of TMAO, sometimes called a "chemical chaperone" (Brown et al., 1996), contrasts those of alcohols such as TFE. TMAO stabilizes compact conformations, and structure is stabilized cooperatively (Baskakov et al., 1999). Furthermore, as shown for proteins destabilized by mutagenesis or covalent modification, the structure stabilized by TMAO is native-like (Baska-

kov & Bolen, 1998). In agreement with these observations, ^{1}H and ^{15}N chemical shifts of native CspA are nearly invariant over the range of TMAO concentrations used in this study.

Protein stability depends on the free energy difference between native and denatured states. The stabilizing effects of TMAO are believed to result from a small increase in the free energy of the native state, coupled with a much larger increase in the free energy of the denatured state (Lin & Timasheff, 1994; Liu & Bolen, 1995; Wang & Bolen, 1997). This is illustrated in Figure 8. A corollary of this mechanism is that the increased protection from solvent exchange observed in the presence of TMAO should reflect changes in the properties of the denatured state rather than of the native state. This agrees with the observation that the low protection of strand $\beta5$ is poorly correlated with the distribution of tertiary contacts, and with hydrogen bonding partners in the native structure. The low stability to exchange of amide protons from strand $\beta5$ is suggestive of conformations in which this strand is segmen-
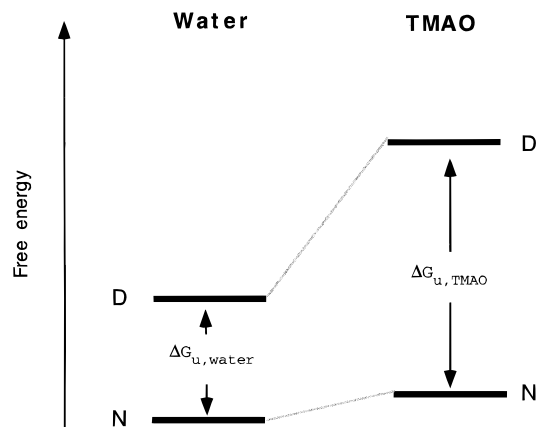


**Fig. 8.** Free energy diagram illustrating the effects of TMAO on protein stability (Lin & Timasheff, 1994).

tally uncoupled from the rest of the structure. Conversely, the strong protection of amide protons in strands $\beta 1$–$\beta 4$ points to a residual shielding from solvent exchange when hydrogen-bonding interactions between strands $\beta 1$–$\beta 4$ and $\beta 5$ are broken. That TMAO leads to increased protection throughout the molecule suggests that the free energies of both partially and globally unfolded species are increased, making exchange susceptible conformations less accessible from the native state.

Solution transfer free energy measurements suggest that the peptide backbone is the dominant factor in the stabilization of proteins by TMAO (Liu & Bolen, 1995; Wang & Bolen, 1997). Favorable interactions between TMAO and amino acid side chains promote denaturation; highly unfavorable interactions between TMAO and the exposed peptide backbone of the unfolded protein strongly oppose denaturation (Wang & Bolen, 1997). This contrasts with protein unfolding in water, which is strongly opposed by unfavorable interactions between solvent and exposed nonpolar side chains in unfolded conformations (e.g., the hydrophobic effect). If the stabilizing effects of TMAO are predominantly due to the peptide backbone, stabilization should become increasingly independent of amino acid hydrophobicity with increasing TMAO concentration (Wang & Bolen, 1997). In the range of TMAO concentrations used for this work, protection becomes detectable for amide protons in the weakly hydrophobic strand $\beta 5$ and in the hydrophilic loops flanking the $\beta$-strands (Fig. 6B). The most hydrophobic segments of the protein, however, still show the strongest protection.

## Materials and methods

### Materials

Urea analytical grade was obtained from Bio-RAD Laboratories (Hercules, California). TMAO (98% pure) was from Acros Organics (Fairlawn, New Jersey). To exchange residual $H_2O$, TMAO was lyophilized twice from 99.98% $D_2O$ solutions. CspA was expressed in *E. coli* using the pET11-*cspA* vector and purified using a published method (Chatterjee et al., 1993), with the modification that cells were grown in MOPS media supplemented with $^{15}NH_4Cl$ (1 g/L) to prepare $^{15}N$ labeled protein (Alexandrescu & Rathgeb-Szabo, 1999).

### Circular dichroism

Unfolding transitions were measured on a Jasco J720 spectropolarimeter at 222 nm. The CD data were recorded at 5 °C, using a 1 mm path length cuvette to minimize interference from urea. Each ellipticity measurement was the average of three data points recorded over 20 s using a 1.5 nm bandwidth. A 20 mM acetic acid/99.8% $D_2O$ buffer was used for the measurements at pD 4.5 and 5.4; 20 mM potassium phosphate/99.8% $D_2O$ was used for pD 7.2. For each pD value, a set of 21–25 samples of 35 $\mu$M CspA were prepared by diluting aliquots from two 2 mM CspA stock solutions in 0 M or 10 M urea, to the desired concentration of urea. Urea concentrations were verified by refractive index measurements (Pace, 1986). Samples were incubated overnight at 5 °C prior to measurements.

### Hydrogen exchange kinetics monitored by NMR

NMR data were recorded on a Bruker DMX spectrometer operating at 500 MHz. Freshly dissolved ~1 mM CspA solutions in ~0.275 mL of 99.98% $D_2O$ were kept on ice prior to measurements, transferred into 5 mm susceptibility-matched tubes (Shigemi, Allison Park, Pennsylvania), and inserted into the NMR probe pre-equilibrated to a temperature of 5 °C. Typically, the time between sample preparation and the start of NMR data acquisition was ~10 min. Backbone amide proton exchange was monitored with sensitivity-enhanced gradient $^1H$-$^{15}N$ HSQC experiments (Kay et al., 1992), recorded as a function of incubation time in $D_2O$. For each urea and TMAO concentration, 14 to 21 time points were used to characterize exchange rates. HSQC spectra were acquired with 2,048* × 100* points, and spectral widths of 8,000 Hz ($^1H$) × 1,900 Hz ($^{15}N$).

### NMR data analysis

$^1H$–$^{15}N$ NMR assignments for CspA were based on the published chemical shift values of Feng et al. (1998). Titration experiments (varying temperature and pH) were used to correlate the assignments obtained at pH 6.0 and 30 °C, with the conditions of the present study (pH 5.4, 5 °C). Hydrogen exchange was characterized by the decay of $^1H$-$^{15}N$ HSQC cross-peak intensities as a function of exchange time, defined as the period from the insertion of the sample into the NMR probe until the end of each HSQC experiment. To compensate for possible chemical shift variations during the course of the HX experiment, cross-peak intensities were calculated using a macro written for Felix 97 (Molecular Simulations, Burlington, Massachusetts), which returns the maximum intensity within a window of 6 × 6 points centered around the cross-peak position in the first HSQC spectrum. The same procedure with a window of 50 × 20 points was used to determine the average absolute intensities in four regions of each spectrum devoid of cross peaks. The mean of these values was taken as the baseline noise and subtracted from the raw cross-peak intensities. Rate constants for exchange were obtained from nonlinear least-squares fits of cross-peak intensity decays as a function of time to the exponential function:

$$I = I_o \exp(-k_{ex} t) \tag{8}$$

using the program DASHA (Orekhov et al., 1995). The initial intensity $I_o$ and the observed exchange rate $k_{ex}$ were treated as free variables in the fit. Uncertainties in the $k_{ex}$ parameters were taken as the standard errors of the fits. Apparent free energies for exchange, $\Delta G_{HX}$, were calculated using observed exchange rates, and intrinsic exchange rates modeled according to Bai et al. (1993). The urea dependence of $\Delta G_{HX}$ was fitted to both of the models specified by Equations 6 and 7. The $F$-test on the limiting ratio of the reduced sum of squared errors (Shoemaker et al., 1981) was used to determine whether the model with the higher number of degrees of freedom (Equation 7) gave a significantly better fit of the data.

### GNM analysis and hydrophobicity plots

Gaussian network model (GNM) calculations were performed as described (Bahar et al., 1998), using a program written in *C* (available from V.A.J.). The 2 Å crystal structure of CspA (Protein Data Bank (PDB) entry 1MJC) and the first model of the CspA NMR structure (PDB entry 3MEF) were used as input for the calculations. Hydrophobicity scores for the sequence of CspA were calculated with the ProtScale module of the ExPASy molecular biology server [http://www.expasy.ch/cgi-bin/protscale.pl]. The amino acid

scale of Kyte & Doolittle (1982) was used, with averaging over a window of seven residues.

## Acknowledgments

## References

Alexandrescu AT, Jaravine VA, Dames SA, Lamour FP. 1999. NMR hydrogen exchange of the OB-fold protein LysN as a function of denaturant: The most conserved elements of structure are the most stable to unfolding. *J Mol Biol 289*:1041–1054.

Alexandrescu AT, Rathgeb-Szabo K. 1998. NMR assignments for acid-denatured cold shock protein A. *J Biomol NMR 11*:461–462.

Alexandrescu AT, Rathgeb-Szabo K. 1999. An NMR investigation of solution aggregation reactions preceding the misassembly of acid denatured cold shock protein A into fibrils. *J Mol Biol 291*:1191–1206.

Anfinsen C. 1973. Principles that govern the folding of protein chains. *Science 181*:223–230.

Bahar I, Wallqvist A, Covell DG, Jernigan RL. 1998. Correlation between native-state hydrogen exchange and cooperative residue fluctuations from a simple model. *Biochemistry 37*:1067–1075.

Bai Y, Englander SW. 1996. Future directions in folding: The multi-state nature of protein structure. *Proteins 24*:145–151.

Bai Y, Milne JS, Mayne L, Englander SW. 1993. Primary structure effects on peptide group hydrogen exchange. *Proteins 17*:75–86.

Bai Y, Milne JS, Mayne L, Englander SW. 1994. Protein stability measured by hydrogen exchange. *Proteins 20*:4–14.

Bai Y, Sosnick TR, Mayne L, Englander SW. 1995. Protein folding intermediates studied by native-state hydrogen exchange. *Science 269*:192–197.

Baskakov I, Bolen DW. 1998. Forcing thermodynamically unfolded proteins to fold. *J Biol Chem 273*:4831–4834.

Baskakov I, Kumar R, Sirnivasan G, Ji Y, Bolen DW, Thompson EB. 1999. Trimethylamine N-oxide-induced cooperative folding of an intrinsically unfolded transcription-activating fragment of human glucocorticoid receptor. *J Biol Chem 274*:10693–10696.

Brown CR, Hong-Brown LQ, Biwersi J, Verkman AS, Welch WJ. 1996. Chemical chaperones correct the mutant phenotype of the delta F508 cystic fibrosis transmembrane conductance regulator protein. *Cell Stress Chaperones 1*:117–125.

Chamberlain AK, Handel TM, Marqusee S. 1996. Detection of rare partially folded molecules in equilibrium with the native conformation of RNase H. *Nat Struct Biol 3*:782–787.

Chamberlain AK, Marqusee S. 1998. Molten globule unfolding monitored by hydrogen exchange in urea. *Biochemistry 37*:1736–1742.

Chatterjee S, Jiang W, Emerson SD, Inouye M. 1993. The backbone structure of the major cold-shock protein CS7.4 of *Escherichia coli* in solution includes extensive β-sheet structure. *J Biochem 114*:663–669.

Clarke J, Fersht AR. 1996. An evaluation of the use of hydrogen exchange at equilibrium to probe intermediates on the folding pathway. *Fold Des 1*:243–254.

Clarke J, Itzhaki LS, Fersht AR. 1997. Hydrogen exchange at equilibrium: A short cut for analysing protein-folding pathways? *TIBS 22*:284–287.

Dill KA, Chan HS. 1997. From Levinthal to pathways to funnels. *Nat Struct Biol 4*:10–19.

Feng W, Tejero R, Zimmerman DE, Inouye M, Montelione GT. 1998. Solution NMR structure and backbone dynamics of the major cold shock protein (CspA) from *Escherichia coli*: Evidence of conformational dynamics in the single-stranded RNA-binding site. *Biochemistry 37*:10881–10896.

Fersht AR. 1997. Nucleation mechanisms in protein folding. *Curr Opin Struct Biol 7*:3–9.

Foord RL, Leatherbarrow RJ. 1998. Effect of osmolytes on the exchange rates of backbone amide protons in proteins. *Biochemistry 37*:2969–2978.

Fuentes EJ, Wand AJ. 1998. Local dynamics and stability of apocytochrome $b_{562}$ examined by hydrogen exchange. *Biochemistry 37*:3687–3698.

Harrison SC, Durbin R. 1985. Is there a single pathway for the folding of a polypeptide chain? *Proc Natl Acad Sci 82*:4028–4030.

Itzhaki LS, Neira JL, Fersht AR. 1997. Hydrogen exchange in chymotrypsin inhibitor 2 probed by denaturant and temperature. *J Mol Biol 270*:89–98.

Jackson SE. 1998. How do small single-domain proteins fold? *Fold Des 3*:R81–R91.

Jiang W, Hou Y, Inouye M. 1997. CspA, the major cold shock protein (CspA) from *Escherichia coli*, is an RNA chaperone. *J Biol Chem 272*:196–202.

Kay LE, Keifer P, Saarinen T. 1992. Pure absorption gradient enhanced heteronuclear single quantum correlation spectroscopy with improved sensitivity. *J Am Chem Soc 114*:10663–10665.

Kraulis PJ. 1991. MOLSCRIPT—A program to produce both detailed and schematic plots of protein structure. *J Appl Crystallogr 24*:946–950.

Kyte J, Doolittle RF. 1982. A simple method for displaying the hydropathic character of a protein. *J Mol Biol 157*:105–132.

Lin T, Timasheff SN. 1994. Why do some organisms use a urea-methylamine mixture as an osmolyte? Thermodynamic compensation of urea and trimethylamine *N*-oxide interactions with protein. *Biochemistry 33*:12695–12701.

Liu Y, Bolen DW. 1995. The peptide backbone plays a dominant role in protein stabilization by naturally occurring osmolytes. *Biochemistry 34*:12884–12891.

Murzin AG. 1993. OB (oligonucleotide/oligosaccharide binding)-fold: Common structural and functional solution for non-homologous sequences. *EMBO J 12*:861–867.

Murzin AG, Brenner SE, Hubbard T, Chothia C. 1995. SCOP: A structural classification of proteins database for the investigation of sequences and structures. *J Mol Biol 247*:536–540.

Orekhov VY, Nolde DE, Golovanov AP, Korzhnev DM, Arseniev AS. 1995. Processing of heteronuclear NMR relaxation data with the new software DASHA. *Appl Magn Reson 9*:581–588.

Pace CN. 1986. Determination and analysis of urea and guanidine hydrochloride denaturation curves. *Methods Enzymol 131*:266–280.

Perl D, Welker C, Schindler T, Schröder K, Marahiel MA, Jaenicke R, Schmid FX. 1998. Conservation of rapid two-state folding in mesophilic, thermophilic, and hyperthermophilic cold shock proteins. *Nat Struct Biol 5*:229–235.

Reid KL, Rodriguez HM, Hillier BJ, Gregoret LM. 1998. Stability and folding properties of a model β-sheet protein, *Escherichia coli* CspA. *Protein Sci 7*:470–479.

Schindelin H, Jiang W, Inouye M, Heinemann U. 1994. Crystal structure of CspA, the major cold shock protein of *Escherichia coli*. *Proc Natl Acad Sci 91*:5119–5123.

Schindler T, Herrler M, Marahiel MA, Schmid FX. 1995. Extremely rapid protein folding in the absence of intermediates. *Nat Struct Biol 2*:663–673.

Schindler T, Schmid FX. 1996. Thermodynamic properties of an extremely rapid protein folding reaction. *Biochemistry 35*:16833–16842.

Shoemaker DP, Garland CW, Steinfeld JI, Nibler JW. 1981. Least-squares fitting procedures. *Experiments in physical chemistry*. New York: McGraw-Hill. pp 728–729.

Tanford C. 1978. The hydrophobic effect and the organization of living matter. *Science 200*:1012–1018.

Wang A, Bolen DW. 1997. A naturally occurring protective system in urea-rich cells: Mechanism of osmolyte protection in proteins against urea denaturation. *Biochemistry 36*:9101–9108.

Wang A, Robertson AD, Bolen DW. 1995. Effects of a naturally occurring compatible osmolyte on the internal dynamics of Ribonuclease A. *Biochemistry 34*:15096–15104.

Wolffe AP. 1994. Structural and functional properties of the evolutionary ancient Y-box family of nucleic acid binding proteins. *Bioessays 16*:245–251.

Yancey PH, Clark ME, Hand SC, Bowlus RD, Somero GN. 1982. Living with water stress: Evolution of osmolyte systems. *Science 217*:1214–1222.

Yi Q, Scalley ML, Simons KT, Gladwin S, Baker D. 1997. Characterization of the free energy spectrum of peptostreptococcal protein L. *Fold Des 2*:271–280.

Zhou H, Wang L. 1996. Chaos in biomolecular dynamics. *J Phys Chem 100*:8101–8105.